applied optics

Electrically controlled spatial-polarization switch based on patterned photoalignment of nematic liquid crystals

ELENA A. MELNIKOVA,[1] ALEXEI L. TOLSTIK,[1] IRINA I. RUSHNOVA,[1,*] OLGA S. KABANOVA,[1] AND ALEXANDER A. MURAVSKY[2]

[1]Physics Department, Belarusian State University, Nezavisimosti Avenue 4, 220030 Minsk, Belarus
[2]Institute of Chemistry of New Materials, National Academy of Sciences, Fr. Skaryna Street 36, 220141 Minsk, Belarus
*Corresponding author: Rushnova@bsu.by

Received 20 April 2016; revised 22 July 2016; accepted 22 July 2016; posted 22 July 2016 (Doc. ID 263520); published 10 August 2016

A switching scheme for two orthogonal modes of laser radiation that is based on the total internal reflection effect realized at the interface of two liquid crystal regions with orthogonal director orientations is proposed. To create the photorefractive interface within the bulk of a liquid crystal, an original technique based on self-alignment of azo dye photoalignment and absorbing electrode patterns has been developed. Spatial separation of the orthogonally polarized light beams and their switching (when the positions of reflected and transmitted light beams are switched) due to the voltage applied has been experimentally realized.

OCIS codes: (230.0230) Optical devices; (230.1360) Beam splitters; (230.3720) Liquid-crystal devices.

http://dx.doi.org/10.1364/AO.55.006491

1. INTRODUCTION

Liquid crystals (LC) exhibiting numerous unique properties attract the attention of researchers both in the field of basic science and in innovative applications far beyond the widely used LC displays (LCD) [1]. At the present time, nematic liquid crystals (NLC) are well known because of their extensive use for the control of light beams due to high index anisotropy (~0.1–0.4), the value of which may be controlled by the application of low voltages (~1–10 V). LC technology, the key innovation of present display and photonic devices, is widely used in mass-produced imaging systems, optical switches, and space–time light modulators featuring low power consumption [2–4].

Other applications are associated with diffraction of laser radiation by the spatially modulated LC structures [5,6], and also with the use of LC cells to generate optical vortexes [7] to produce the electrically switchable Fresnel lens [8] or to transform linearly polarized light beams into beams with a radial or azimuthal polarization [9]. Regularly, in planar LC cells comprising two glass substrates and a LC layer between them, light beams are directed perpendicular to the substrates. New possibilities are offered by the optical schemes, where a light field is propagated within a LC layer along the glass substrates [10,11]. Of particular interest are photonic LC structures with complex optical anisotropy based on innovative patterned photoalignment materials [12–14]. Such elements may be used in fiber-optical communication lines, data processing, and in devices of integrated optics (compact optoelectronic switches of light beams, waveguides, dividers, and adders) [15,16]. Their operation is based on the effect of light refraction and reflection from the interface of two LC regions with the orthogonal director orientations [17–19]. By analysis of various combinations of the orthogonal NLC director orientations, the optimum configurations have been established for realization of the total internal reflection (TIR) effect of the linearly polarized light beams [20]. Using the two interfaces of LC regions having orthogonal director orientations, one can design LC waveguides to implement the waveguide propagation of laser radiation [21,22].

This paper presents a new topological scheme for LC director orientation on the basis of an original technique with the use of azo dye as a photosensitive alignment material. The manufactured electrically controlled LC elements offer not only the possibility to separate spatially the orthogonally polarized light beams, but also to realize their switching when the positions of reflected and transmitted beams are changed over, in fact operating as an active reflective polarizer.

2. LC CELL STRUCTURE AND PRINCIPLE OF WORK

A typical schematic of the electrically controlled LC element (sandwich-type cell) is shown in Fig. 1.

Fig. 1. Structure of a LC cell.

A nontransparent layer of chromium deposited on the lower glass substrate serves as an electrode. To form the electrically controllable interface between two regions of LC, the nontransparent electrode was etched from half of the substrate. A transparent electrode of indium tin oxide (ITO) forms a conducting layer on the upper substrate. Owing to the transparent electrode, there is a possibility to record the electromagnetic radiation propagation pattern in the LC element by fixing the scattered radiation at inhomogeneities in the LC director orientation [22]. The photoalignment technique is used to set the required initial orientation of the LC molecules [23–25]. The photosensitive alignment material is represented by the water-insoluble azo dyes (3), synthesized at the Institute of Chemistry of New Materials of the Belarusian National Academy of Sciences, which are characterized by high anchoring energy, thermostability, photostability, and insensitivity to moisture treatment [26]. Under the effect of polarized light, the dye layer forms a linear molecular structure that aligns the LC. The azo dye molecular orientation is effected by illumination with the help of blue-light-emitting diodes at the wavelength peak 457 nm. By the choice of alignment material sensitive to blue light within the visible range, the fabrication cost of patterned photoaligned LC cells with standard STN glass is significantly reduced, owing cheaper integrated LC photonic elements for red and NIR light, in comparison with quartz substrates and UV photoalignment. The unique feature of the proposed fabrication technique is the self-alignment of the liquid crystal orientation directions on the upper and lower substrates achieved in two-step polarized light exposures performed after LC cell assembly. The first step: the assembled cell is exposed from the side of the ITO electrode, giving uniform azimuthal LC orientation at both substrates. An optional second step: the cell is exposed from the side of a chromium electrode, acting as a self-aligned photomask. The thickness of the LC layer is controlled by 20 μm spacers. The cell was filled with positive birefringent NLC having a refractive index anisotropy $\Delta n = 0.18$; the threshold voltage for realignment of the NLC director orientation was $U_{\mathrm{tr}} = 1$ V.

The initial orientation of the LC director has been considered in the three geometries (see Fig. 2) associated with a homogeneous planar director orientation along the interface between two regions (a, $U = 0$), homogeneous planar orientation of the director perpendicular to the interface of the two regions (b, $U = 0$), or planar mutually orthogonal director orientations in adjacent regions of the LC cell (c, $U = 0$).

When the applied electric field is above the threshold ($U \gg U_{\mathrm{tr}}$), reorientation of the director from the initial planar to the vertical alignment occurs, due to the Fredericks transition [27], in the LC cell region in-between two electrodes. It should be noted that the interfaces for the two LC director orientations given in Figs. 2(a) and 2(b) and observed with the applied electric field make it possible to design a LC

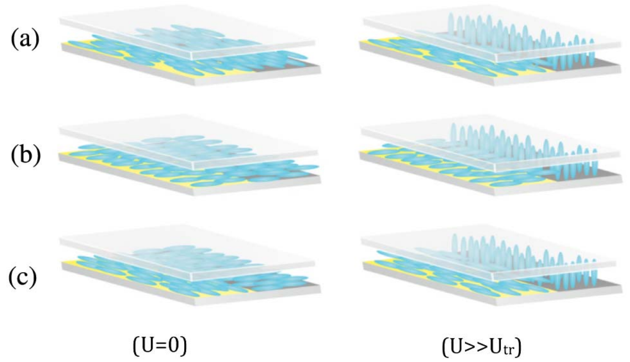

Fig. 2. Schematic of the interfaces between two regions of NLC with the orthogonal director orientations.

element with the controllable interface of LC domains for separation of two orthogonally polarized modes [21]. The third geometry [see Fig. 2(c)] is original: mutually orthogonal orientations of the LC director occur both without and with the use of an external electric field.

Figure 3 schematically demonstrates the propagation of linearly polarized radiation within a NLC layer with such a refractive interface.

To realize the spatial-polarization switching, a light beam is injected into the LC element from the cell face at the angle θ to the interface between two domains of LC. As seen in Fig. 3, the interface between two LC domains with mutually orthogonal planar orientations of the director exists without any electric field applied. In this case the refractive index of vertically polarized (perpendicular to the cell plane) radiation is independent of the light beam propagation direction; for both domains of LC it is determined by the index of an ordinary wave n_o. The light beam with such polarization is insensitive to the interface of the two domains, propagating within the LC cell without any changes of its direction for every angle of incidence on the interface.

For a light beam horizontally polarized within the cell plane, the indices in both domains of LC are different, being determined by a relative orientation of the LC director and of the light-wave electric vector [20]. To illustrate, for the case of a light beam polarized horizontally [Fig. 3(a)], the index in the first domain (where the light beam is entering the LC cell) may be found from the following expression:

$$n_{1\mathrm{ef}}(\theta) = \frac{n_e n_o}{\sqrt{n_e^2 \sin^2\theta + n_o^2 \cos^2\theta}}, \tag{1}$$

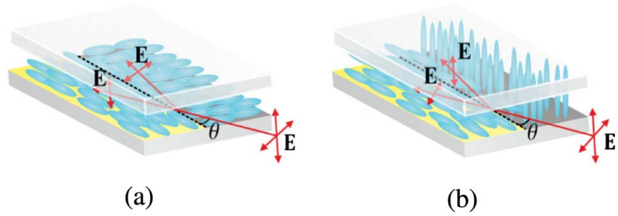

Fig. 3. Schematic of the propagation of linearly polarized radiation in the LC cell having the refractive interface without (a, $U = 0$) and with (b, $U \gg U_{\mathrm{tr}}$) the electric field applied.

where θ is the angle between the LC director and the light-wave electric vector, that in this case is coincident with the angle between the wave vector and the photorefractive interface.

In the second domain of LC, due to rotation of the director by 90°, the refractive index is the next:

$$n_{2\mathrm{ef}}(\theta) = \frac{n_e n_o}{\sqrt{n_e^2 \cos^2\theta + n_o^2 \sin^2\theta}}. \tag{2}$$

The difference in the refractive indices of the two LC domains leads to refraction and reflection of a light beam by the interface between these domains, as distinct from the vertically polarized light beam, for which there is no such an interface. Note that in the case $n_{1\mathrm{ef}}(\theta) > n_{2\mathrm{ef}}(\theta)$, the fulfillment of the total internal reflection condition is expected.

Considering expressions (1) and (2) for the indices, we can write an equation for the propagation critical angle θ_{TIR} meeting the TIR effect:

$$\cos\theta_{\mathrm{TIR}} = \frac{n_{2\mathrm{ef}}(\theta_{\mathrm{TIR}})}{n_{1\mathrm{ef}}(\theta_{\mathrm{TIR}})}, \tag{3}$$

giving the following solution:

$$\theta_{\mathrm{TIR}} = \arccos\sqrt{\frac{\sqrt{5n_e^4 - 4n_o^2 n_e^2} - n_e^2}{2(n_e^2 - n_o^2)}}. \tag{4}$$

For NLC used in this work (with the refractive index of an ordinary wave $n_o = 1.49$ and of an extraordinary wave $n_e = 1.67$), possible propagation angles associated with the TIR effect are given by the relation:

$$\theta \le \theta_{\mathrm{TIR}} \approx 23°. \tag{5}$$

With the application of an electric field exceeding the threshold ($U \gg U_{\mathrm{th}}$), in the LC cell region with two electrodes the director is realigned: the initial (planar) LC alignment is switched to vertical; whereas in the adjacent region the initial orientation of the director is retained. In this case the refractive indices for horizontally polarized light are given as follows:

$$n_1 = n_o, \tag{6}$$

$$n_2(\theta) = \frac{n_e n_o}{\sqrt{n_e^2 \cos^2\theta + n_o^2 \sin^2\theta}}. \tag{7}$$

As $n_2(\theta) > n_1$, the refraction effect is observed for horizontally polarized light. For light with vertical polarization, we have

$$n_1 = n_e, \tag{8}$$

$$n_2 = n_o, \tag{9}$$

and the TIR effect occurs for the angles smaller than the critical angle

$$\theta \le \theta_{\mathrm{TIR}} = \arccos\frac{n_0}{n_e} \approx 26,8°. \tag{10}$$

In this way, when an electric field is applied, the optical properties of the refractive interface between two regions of LC are changed for linearly polarized light. Without the external field, TIR is possible for horizontally polarized light (in the cell plane); but with the field applied, TIR is possible for vertically polarized light.

When nonpolarized radiation is incident on the interface between two LC regions with orthogonal orientations of the director, the beam will be divided into two separate components. For one of the components, the total internal reflection will be observed, whereas the other one is subjected to refraction on passing through the interface. The lower the angle between the incident beam and the refractive interface, the higher the amount of light falling within the TIR conditions.

3. EXPERIMENTAL RESULTS AND DISCUSSION

The theoretical estimations above were experimentally verified and applied for the development of an electrically controlled spatial-polarization LC switch. On the inner surfaces of the glass cell, the azo dye photoalignment material was applied (Fig. 1). The initial planar molecular orientation of LC in two mutually orthogonal directions within the cell plane was set by the two-step exposure. First the cell was illuminated from the side of a transparent electrode to provide homogeneous illumination with polarized light to specify the direction of azo dye photoalignment. Then the cell was additionally illuminated using orthogonally polarized light from the other side. As half of the cell was under the nontransparent chromium electrode, the in-cell LC alignment direction is changed only in the nonmasked region. Finally the cell was filled with NLC and two LC domains with orthogonal planar orientations of the director were formed.

Figure 4 schematically shows an experimental setup for polarization switching.

Radiation of He–Ne laser 1 with the wavelength $\lambda = 633$ nm and the second harmonic radiation of Nd:YAG laser 2 with the wavelength $\lambda = 532$ nm were attenuated by optical filters 3, 4 down to the power $P = 0.3$ mW. Wire grid polarizer 5 and diaphragm 6 offered the propagation of two orthogonally polarized light beams at different wavelengths in the same path (horizontally polarized radiation of a He–Ne laser and vertically polarized second-harmonic radiation of a Nd:YAG laser). The light beams focused by 10X lens 7 were incident on the face of LC element 9 mounted at the rotary X–Y–Z stage 8 that enabled one to control the radiation input angle into the LC element. Laser radiation was input at an angle of 15° to the refractive interface. The waist diameter at the input into the LC element was ≈20 μm. The propagation of light beams within the LC layer was recorded by the light

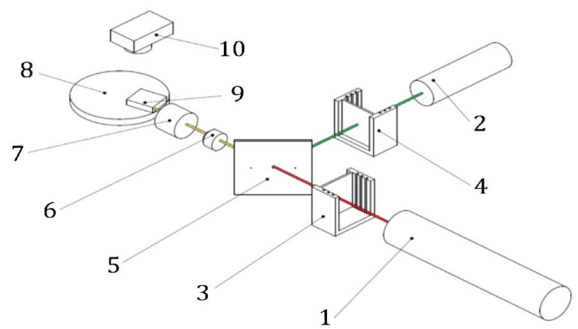

Fig. 4. Experimental setup: 1) He–Ne laser, 2) Nd:YAG laser, 3,4) attenuation filters, 5) wire grid polarizer, 6) diaphragm, 7) lens, 8) X–Y–Z stage, 9) LC element, 10) CCD camera.

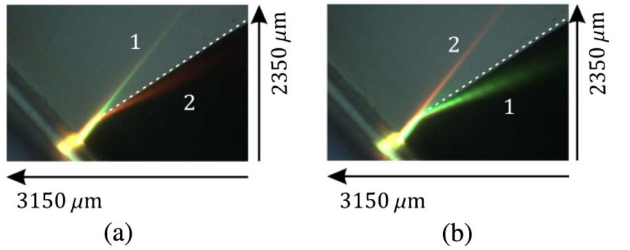

Fig. 5. Switching effect of orthogonally polarized light beams in the electrically controlled LC cell with the refractive interface (1—second harmonic radiation of a Nd:YAG laser, 2—radiation of a He–Ne laser) without (a, $U = 0$) and with (b, $U = 3.5$ V) the electric field applied.

scattered from the LC inhomogeneities with the use of Point Grey CCD camera 10 positioned above LC cell 9. The CCD camera was integrated with a 8X lens making it possible to record the area with the dimensions 3150 × 2350 μm at the resolution 1280 × 960 pixels.

Figure 5 presents the experimental photographs illustrating the operation of an electrically controlled spatial-polarization switch. It is seen that, without the applied electric field [Fig. 5(a), $U = 0$], horizontally polarized radiation of a He–Ne laser is reflected, whereas the vertically polarized second-harmonic radiation of a Nd:YAG laser is passing the interface (dashed line) without any changes in its propagation direction. Indeed, for horizontally polarized radiation, the refractive indices are as follows: $n_{1ef}(\theta) = 1.656$, $n_{2ef}(\theta) = 1.500$; the critical radiation incidence angle on the interface is $\theta_{TIR} = 25°$. With the applied field [Fig. 5(b), $U = 3.5$ V], the situation is opposite. In this case the vertically polarized second-harmonic radiation of a Nd:YAG laser meets the TIR condition ($n_1(\theta) = 1.6557$, $n_2 = 1.49$, $\theta_{TIR} = 25.85°$), whereas horizontally polarized radiation of a He–Ne laser is propagating practically along the straight line. As indicated by the numerical estimates, for the selected experimental scheme ($n_1(\theta) = 1.504$, $n_2(\theta) = 1.500$), the difference between the angle of refraction and the incidence angle is 0.58° only.

4. CONCLUSION

To conclude, in this paper a new geometry of an integrated LC photonic element with an electrically controlled interface between two regions of orthogonal LC director orientations is proposed. Innovative self-alignment fabrication and patterned photoalignment techniques were implemented for experimental realization of polarization switching of light beams in a voltage controlled LC photonic device based on the TIR effect. The distinctive features of this scheme are the possibility for spatial separation of the polarization components of laser radiation and the ability of its spatial switching when the propagation paths of two orthogonally polarized light beams are switched over.

Funding. Belarusian Republican Foundation for Fundamental Research ("Convergence-2020" 3.03.5).

REFERENCES

1. J. P. F. Lagerwall and G. Scalia, "A new era for liquid crystal research: applications of liquid crystals in soft matter nano-, bio- and microtechnology," Curr. App. Phys. **12**, 1387–1412 (2012).
2. A. Georgiou, J. Christmas, J. Moore, A. Jeziorska-Chapman, A. Davey, N. Collings, and W. A. Crossland, "Liquid crystal over silicon device characteristics for holographic projection of high-definition television images," Appl. Opt. **47**, 4793–4803 (2008).
3. P. Xu, V. Chigrinov, and H.-S. Kwok, "Optical analysis of a liquid-crystal switch system based on total internal reflection," J. Opt. Soc. Am. A **25**, 866–873 (2008).
4. J. P. Parry, R. J. Beck, J. D. Shephard, and D. P. Hand, "Application of a liquid crystal spatial light modulator to laser marking," Appl. Opt. **50**, 1779–1785 (2011).
5. A. A. Kazak, E. A. Melnikova, A. L. Tolstik, U. V. Mahilny, and A. I. Stankevich, "Controlled diffraction liquid-crystal structures with a photoalignment polymer," Tech. Phys. Lett. **34**, 861–863 (2008).
6. H. Sarkissian, S. V. Serak, N. V. Tabiryan, L. B. Glebov, V. Rotar, and B. Y. Zeldovich, "Polarization-controlled switching between diffraction orders in transverse-periodically aligned nematic liquid crystals," Opt. Lett. **31**, 2248–2250 (2006).
7. A. S. Ostrovsky, C. Rickenstorff-Parrao, and V. Arrizón, "Generation of the 'perfect' optical vortex using a liquid-crystal spatial light modulator," Opt. Lett. **38**, 534–536 (2013).
8. A. A. Kazak, A. L. Tolstik, and E. A. Mel'nikova, "Controlling light fields by means of liquid-crystal diffraction elements," J. Opt. Technol. **77**, 461–462 (2010).
9. A. A. Kazak, A. L. Tolstik, E. A. Melnikova, and A. A. Komar, "Operation with laser radiation by using of liquid crystal elements," Nonlinear Phenom. Complex Syst. **16**, 302–308 (2013).
10. J. Beeckman, K. Neyts, X. Hutsebaut, C. Cambournac, and M. Haelterman, "Simulations and experiments on self-focusing conditions in nematic liquid-crystal planar cells," Opt. Express **12**, 1011–1018 (2004).
11. R. Barboza, A. Alberucci, and G. Assanto, "Electro-optic beam steering with nematicons," Mol. Cryst. Liq. Cryst. **558**, 12–21 (2012).
12. J. Beeckman, K. Neyts, and P. Vanbrabant, "Liquid-crystal photonic applications," Opt. Eng. **50**, 081202 (2011).
13. A. Muravsky, *Next Generation of Photoalignment* (VDM Verlag Dr. Müller, 2009).
14. V. G. Chigrinov, *Liquid Crystal Photonics: Engineering Tools, Techniques and Tables* (Nova Science, 2014).
15. S. V. Serak, N. V. Tabiryan, M. Peccianti, and G. Assanto, "Spatial soliton all-optical logic gates," IEEE Photon. Technol. Lett. **18**, 1287–1289 (2006).
16. O. S. Kabanova, E. A. Melnikova, I. I. Olenskaya, and A. L. Tolstik, "Electrically controlled waveguide liquid-crystal elements," Tech. Phys. Lett. **40**, 598–600 (2014).
17. M. Peccianti, A. Dyadyusha, M. Kaczmarek, and G. Assanto, "Tunable refraction and reflection of self-confined light beams," Nat. Phys. **2**, 737–742 (2006).
18. A. G. Maksimochkin, S. V. Pasechnik, G. I. Maksimochkin, and V. G. Chigrinov, "Electrically controlled waveguide mode in LC layer for fiber optic applications," Opt. Commun. **283**, 3136–3141 (2010).
19. G. Assanto, A. Fratalocchi, and M. Peccianti, "Spatial solitons in nematic liquid crystals: from bulk to discrete," Opt. Express **15**, 5248–5259 (2007).
20. A. Komar, A. Tolstik, E. Melnikova, and A. Muravsky, "Optical switch based on the electrically controlled liquid crystal interface," Appl. Opt. **54**, 5130–5135 (2015).
21. A. A. Komar, M. A. Kurochkina, A. A. Melnikova, A. I. Stankevich, and A. L. Tolstik, "Polarization separation of light beams at the interface of two mesophases," Tech. Phys. Lett. **37**, 704–706 (2011).
22. A. G. Maksimochkin, S. V. Pasechnik, V. A. Tsvetkov, D. A. Yakovlev, G. I. Maksimochkin, and V. G. Chigrinov, "Electrically controlled switching of light beams in the plane of liquid crystal layer," Opt. Commun. **270**, 273–279 (2007).
23. V. Chigrinov, H.-S. Kwok, H. Hasebe, H. Takatsu, and H. Takada, "Liquid-crystal photoaligning by azo dyes," J. Soc. Inf. Disp. **16**, 897–904 (2008).

24. V. S. Mikulich, A. A. Muravsky, A. A. Murauski, I. N. Kukhta, and V. E. Agabekov, “Photoalignment dynamics of azo dyes series with different coordination metals,” J. Soc. Inf. Disp. **22**, 29–34 (2014).
25. V. S. Mikulich, A. A. Muravsky, A. A. Murauski, and V. E. Agabekov, “Effect of cis/trans-isomerisation on photoalignment of azo dyes,” Rus. J. Gen. Chem. **85**, 571–576 (2015).
26. V. Mikulich, A. Murauski, A. Muravsky, V. Agabekov, and V. Bezruchenko, “Waterproof material for liquid crystals photoalignment based on azo dyes,” J. Soc. Inf. Disp. **22**, 199–203 (2014).
27. L. M. Blinov, *Electrooptical and Magnetooptical Properties of Liquid Crystals* (Wiley, 1983).